The effect of metal oxide additives on the activity of V_2O_5/TiO_2 catalysts for the selective catalytic reduction of nitric oxide by ammonia

Michael D. Amiridis[a,*], Robert V. Duevel[b], Israel E. Wachs[c]

[a]Department of Chemical Engineering, University of South Carolina, Columbia, SC 29208, USA
[b]Research Division, W.R. Grace and Co.-Conn., Columbia, MD 21044, USA
[c]Department of Chemical Engineering, Zettlemoyer Center for Surface Studies, Lehigh University, Bethlehem, PA 18015, USA

Abstract

A systematic investigation of the effect of various metal oxides additives on the reactivity of a 1 wt% V_2O_5/TiO_2 catalyst for the selective catalytic reduction (SCR) of NO by NH_3 has been carried out at 623 K. Activity measurements were conducted in a simulated flue gas containing H_2O and SO_2, and indicated that the activity of the V_2O_5/TiO_2 catalyst can be significantly affected by the presence of an additional metal oxide. MoO_3 and WO_3 were found to have the biggest promoting effect, while ZnO was found to have the biggest poisoning effect. The structure of the surface vanadia species, as well as of some of the other transition metal oxides, was characterized by in situ Raman spectroscopy. Ammonia-temperature programmed desorption (NH_3-TPD) was used to probe the reducibility and total acidity of the different catalysts. Diffuse reflectance infrared Fourier transform spectroscopy (DRIFTS) was used to probe the type of the different acid sites on the catalyst surface. The analysis of our results suggests a strong correlation between the SCR activity and the amount of Brønsted acid sites on the catalyst surface. © 1999 Elsevier Science B.V. All rights reserved.

Keywords: Selective catalytic reduction; Nitric oxide; Ammonia; V_2O_5/TiO_2; Promoters; MoO_3; WO_3

1. Introduction

Among the various catalysts studied for the selective catalytic reduction (SCR) of nitric oxide by ammonia, vanadia/titania-based systems are the most active in the temperature range between 573 and 723 K. As a result, they are used widely for the control of NO_x emissions from stationary sources [1–4]. Several mechanisms have been proposed in the literature for the SCR reaction, including both Langmuir–Hinshelwood [5–7] and Eley–Rideal [8–11] type models. The rate determining step, and therefore, the desired characteristics of the active vanadia site continue to be a point of debate. Attempts have been made to correlate the SCR activity of supported V_2O_5 catalysts to the reducibility of the vanadia, hence implying that the reduction of the active vanadia site is involved in the rate determining step for the SCR reaction [12–14]. Others have proposed that surface Brønsted acidity is

---

*Corresponding author. Fax: +1-803-777-8265; e-mail: amiridis@sun.che.sc.edu

the main factor controlling the SCR rate [15–17], and suggested that ammonia activation on a Brønsted acid site is the rate determining step [18]. Recently, Topsøe et al. [11,17] proposed that both steps may be kinetically significant depending on the concentration of O_2.

In addition to their SCR activity, commercial NO_x control catalysts need to satisfy a variety of constraints related to their selectivity for side reactions (such as the oxidation of SO_2 to SO_3), their physical characteristics (such as crush strength and abrasion resistance), and their resistance to poisoning by flue gas trace elements (such as alkali metals, arsenic, etc.). Addition of other metal oxides to the V_2O_5/TiO_2 catalysts has been shown to improve their properties in one or more of these areas, with WO_3 and MoO_3 being the most frequently added in commercial formulations [1–4,19]. Limited information is available in the literature, however, regarding the effect of metal oxide additives on the reactivity of the V_2O_5/TiO_2 catalysts. In addition, the few previous studies available (e.g. [20–24]) have either focused on a single additive, making it difficult to generalize the conclusions, or have been conducted, for simplicity, under conditions significantly different than the ones encountered in commercial applications (i.e. lower temperatures, absence of H_2O and SO_2).

In this work, the effect of various metal oxide additives on the reactivity of V_2O_5/TiO_2 catalysts for the SCR reaction was systematically investigated with a series of samples with constant V_2O_5 (approximately 1.0 wt% or 0.12 mmol of V/g) and additive (approximately 0.35 mmol of metal/g) loadings. Such loadings are typical of commercial catalysts. Similarly, activity measurements were conducted under conditions expected in commercial applications (i.e. 623 K and gas streams containing H_2O and SO_2). The significant differences in the reactivity of the catalysts studied in the presence of metal oxide additives, prompted the initiation of an extensive catalyst characterization effort aimed at understanding the effect of the additives and elucidating the mechanism of the SCR reaction. The structure of the vanadia, as well as of some of the transition metal oxides in the different samples was characterized by in situ Raman spectroscopy. In addition, ammonia temperature programmed desorption (NH_3-TPD) and diffuse reflectance infrared Fourier transform spectroscopy (DRIFTS) of

adsorbed pyridine were utilized to probe both the reduction/oxidation and acidity properties of these catalysts.

2. Experimental

2.1. Catalyst preparation

The catalysts utilized in this study were prepared by the incipient wetness impregnation method. Kemira Grade 907 TiO_2, which had been calcined prior to impregnation, was used as the support. Vanadium citrate was utilized as the precursor of vanadium oxide; ammonium molybdate and metatungstate as the precursors of molybdenum and tungsten oxides; manganous, ferric, lanthanum, cerium and gallium nitrates as the precursors of manganese, iron, lanthanum, cerium and gallium oxides; tin sulfate as the precursor of tin oxide; zinc acetate as the precursor of zinc oxide; germanium chloride as the precursor of germanium oxide; and finally, niobium ethoxide as the precursor of niobium oxide.

Aqueous solutions were used for all the impregnations, with the exception of germanium chloride and niobium ethoxide. Anhydrous alcohol solutions were used in these cases, due to the decomposition of these compounds in water due to hydrolysis. A consecutive impregnation procedure was followed for the preparation of the promoted vanadia catalysts. The vanadia impregnation was the initial step in all cases, and was followed by overnight drying and a 2 h calcination at 773 K, before a second impregnation with the additive. All catalysts were finally dried overnight and calcined at 723 K for 3 h and 793 K for 6 h. It is expected that under such a calcination protocol all precursors will decompose to yield the corresponding metal oxides.

Finally, a second set of samples containing the additive metal oxides, but no vanadia, was prepared for comparison purposes following the same impregnation and calcination protocol.

2.2. Elemental analysis, BET and XRD

Elemental analysis was performed on all samples using an inductively coupled plasma atomic emission spectrometer (ICP-AES) from Applied Research

Table 1
Composition and surface area of various catalysts utilized in this study

Catalyst	V^a	M^b	M^c	SA^d	Catalyst	M^b
V_2O_5/TiO_2	0.63			53		
$V_2O_5–CeO_2/TiO_2$	0.57	4.8	3.4	55	CeO_2/TiO_2	4.5
$V_2O_5–Fe_2O_3/TiO_2$	0.61	2.1	3.8	57	Fe_2O_3/TiO_2	1.9
$V_2O_5–Ga_2O_3/TiO_2$	0.73	2.2	3.2	55	Ga_2O_3/TiO_2	2.2
$V_2O_5–GeO_2/TiO_2$	0.60	2.2	3.0	57	GeO_2/TiO_2	2.4
$V_2O_5–La_2O_3/TiO_2$	0.62	5.3	3.8	54	La_2O_3/TiO_2	6.0
$V_2O_5–MnO_2/TiO_2$	0.64	1.9	3.5	57	MnO_2/TiO_2	2.0
$V_2O_5–MoO_3/TiO_2$	0.61	3.8	4.0	60	MoO_3/TiO_2	3.5
$V_2O_5–Nb_2O_5/TiO_2$	0.65	3.4	3.7	55	Nb_2O_5/TiO_2	3.4
$V_2O_5–SnO_2/TiO_2$	0.66	3.1	2.6	60	SnO_2/TiO_2	3.0
$V_2O_5–WO_3/TiO_2$	0.61	6.3	3.4	56	WO_3/TiO_2	6.2
$V_2O_5–ZnO/TiO_2$	0.73	2.3	3.5	52	ZnO/TiO_2	2.2

[a] Vanadium loading (wt% V).
[b] Additive loading (wt% metal).
[c] Additive loading (moles metal/g catalyst$\times 10^{-4}$).
[d] BET surface area (m^2/g).

Laboratories, (Model 3410). Similarly, the surface area of each sample was determined through BET measurements performed using a Quantochrome Monosorb BET analyzer (Model MS-13). A detailed list of the catalysts employed in this study, along with the results of the elemental analysis and the surface area measurements for each catalyst is shown in Table 1. X-ray diffraction (XRD) patterns were collected with a Philips X-ray powder diffractometer (Model APD 3720). The only peaks detected during the XRD analysis were the ones attributed to anatase TiO_2 from the titania support.

2.3. Activity tests

The activity tests for the selective catalytic reduction of NO by NH_3 were carried out in a stainless steel one pass flow reactor in a simulated flue gas containing 400 ppm NO, 400 ppm NH_3, 4% O_2, 800 ppm SO_2, and 8% H_2O. The reacting gases were mixed and preheated prior to the reactor entrance. Analyzed certified mixtures were used as the sources of the flue gas components. Air was mixed in as the source of O_2, and N_2 as the carrier gas. Water was introduced to the system through a high performance pump (Shimadzu). The catalyst temperature was measured through a thermocouple projecting into the center of the catalyst bed. The NO concentration at both the inlet and outlet of the reactor was analyzed by the use of a chemilu-

minescent analyzer (Thermo Electron). Each run utilized approximately 0.1 g of catalyst in the form of 40/60 mesh spherical particles. The total flow rate over the catalyst was controlled at approximately 3300 standard cm^3/min (200 standard l/h).

2.4. Raman spectroscopy

Raman spectra of the catalysts examined in this study were acquired using a specially designed in situ cell where the temperature and gaseous environment could be controlled. The 514.5 nm line of a 4 W argon-ion laser (Lexel Laser, Model 95) was used as the excitation source; the laser power was 20–25 mW when measured at the sample. The Raman-scattered light from the sample was collected in a back scattering geometry and focused into the last monochromator stage of a 0.64 meter triple monochromator (Instruments SA, Model T64000) equipped with a charge coupled detector (CCD) that was liquid-nitrogen-cooled to 140 K. The Raman spectra were collected and recorded using a computerized data acquisition system (a 386 IBM compatible computer) and software from the instrument manufacturer. For all of the scans, the spectral resolution and reproducibility was experimentally determined to be better than 4 cm^{-1}. The spectral slit width was typically less than 2 cm^{-1} for these measurements. About 0.2–0.3 g of each sample was pressed into a thin wafer of about

1 mm thickness. Each sample was then mounted into a spinning holder and rotated at approximately 600 rpm to avoid local heating effects from the laser radiation.

2.5. Temperature programmed studies

For the NH_3-TPD experiments 30 mg of sample were used and were initially treated for 1 h at 823 K with a 5% O_2/He mixture. The sample was then cooled to 373 K and NH_3 was introduced as a 1000 ppm NH_3/He mixture for 1 h. Following the ammonia adsorption the sample was flashed with 300 cm^3/min He for 1 h to remove any weakly held ammonia. Finally, the He flow was adjusted to 60 cm^3/min and the temperature was ramped at a rate of 20 K/min up to 823 K. Desorption products were monitored through a Hiden quadropole mass spectrometer.

2.6. Diffuse reflectance infrared Fourier transform spectroscopy (DRIFTS)

Pyridine adsorption was performed at 423 K, following an 1 h evacuation of the samples at 823 K. A saturated pyridine in helium mixture was created by passing a helium stream through a pyridine container maintained at 273 K. The samples were exposed to this mixture for 2 h, and then evacuated overnight at 453 K to remove all weakly held pyridine. Pyridine adsorption was performed simultaneously on batches of eight samples, containing at least one "standard" sample (zeolite H–ZSM-5) per batch. The DRIFTS spectra were collected with a Nicolet 60sx instrument equipped with a standard DRIFTS accessory (1 cm^{-1} resolution).

3. Results and discussion

3.1. Effect of additives on SCR activity

Reaction rates were estimated by treating the reactor as a plug flow or integral reactor, according to the following equation

$$r = -(F_{NO}/m_{cat}) \times \ln(1-x) \qquad (1)$$

where r is the reaction rate, F_{NO} the molar feed rate of NO to the reactor, m_{cat} the mass of the catalyst in the reactor, and x is the fractional conversion of NO across the reactor.

This equation assumes a first order dependence on NO and zero order dependence on NH_3, in agreement with previously published results over several V_2O_5-based SCR catalysts ([25] and references therein). More recent reports [26,27] suggest that under certain conditions a fractional NO order in the range 0.7–1.0 may more accurately represent the kinetics of the SCR reaction. The use of such a kinetic order will modify Eq. (1) and will slightly change the rates calculated from it, but will not affect the comparisons and conclusions of our study.

Under our experimental conditions, diffusion limitations were important for some of the catalysts tested. Therefore, intrinsic rates were calculated according to standard correction methods [28]. In particular, the model of Wakao and Smith [29] was used to calculate the effective diffusion coefficients. For similar catalysts, coefficients calculated using this method were found to be within 10% of the experimentally measured values [30]. Experiments repeated with similar catalysts using different particle sizes have shown that the calculated intrinsic rates are within 10%, further validating this correction method [31]. The observed conversions in our study varied between 7% and 50%, while the effectiveness factors varied between 0.5 and 1 (due to the differences in the activity of the catalysts).

The steady state SCR activity of the various promoted V_2O_5/TiO_2 catalysts was measured at 623 K in the presence of H_2O and SO_2. The results of these measurements are summarized in Table 2. The reported activity for the unpromoted V_2O_5/TiO_2 sample is in good agreement with measurements made under similar conditions in our previous studies [32]. As the results in Table 2 show, the presence of the second metal oxide phase has different effects on the SCR activity of the V_2O_5/TiO_2 catalyst depending on the nature of the additive. Thus, some of the metal oxide additives promote the SCR activity (i.e. MoO_3, WO_3 and Nb_2O_5); others have no significant effect on it (i.e. GeO_2, Fe_2O_3 and CeO_2); and finally, others appear to poison it (i.e. MnO_2, Ga_2O_3, La_2O_3, SnO_2 and ZnO).

Limited information is available in the literature regarding the SCR activity of similar catalysts. Our results are in agreement with previous reports regarding the promoting effect of MoO_3, WO_3 [20–22,24,33,34] and the poisoning effect of ZnO [33].

Table 2
SCR activity of various promoted V_2O_5/TiO_2 catalysts at 623 K
(400 ppm NO, 400 ppm NH_3, 4% O_2, 800 ppm SO_2, 8% H_2O)

Catalyst	R_{obs}[a]	R_{int}[b]
V_2O_5–MoO_3/TiO_2	5.9	11.1
V_2O_5–WO_3/TiO_2	5.2	8.7
V_2O_5–Nb_2O_5/TiO_2	3.8	5.0
V_2O_5–GeO_2/TiO_2	3.4	4.6
V_2O_5–Fe_2O_3/TiO_2	3.5	4.5
V_2O_5/TiO_2	3.2	4.2
V_2O_5–CeO_2/TiO_2	2.9	3.2
V_2O_5–MnO_2/TiO_2	2.2	2.5
V_2O_5–Ga_2O_3/TiO_2	2.2	2.5
V_2O_5–La_2O_3/TiO_2	2.0	2.3
V_2O_5–SnO_2/TiO_2	1.6	1.8
V_2O_5–ZnO/TiO_2	0.7	0.7

[a]Observed rate [(μmol NO)/(g catalyst) (s)].

[b]Intrinsic rate [μmol NO)/(g catalyst)(s)].

Furthermore, it has been reported that MoO_3/TiO_2 and WO_3/TiO_2 are active SCR catalysts even in the absence of V_2O_5 [35–38], but their activity is significantly lower than that of V_2O_5/TiO_2 [36,38], and hence, cannot account for the two to three fold increase observed with the V_2O_5–MoO_3/TiO_2 and V_2O_5–WO_3/TiO_2 systems. On the contrary, Weng and Lee [23] have reported that under conditions similar to the ones employed in our work, the addition of Nb_2O_5 to a V_2O_5/TiO_2 catalyst decreases the SCR rate. However, the amount of vanadia contained in the catalyst examined in that study was in excess of two theoretical monolayers. Under such conditions vanadia is expected to be in a crystalline form [24,39] and its catalytic behavior could be different from the behavior of the dispersed vanadia present in our samples, which is typical of commercial SCR catalysts.

3.2. Vanadia structure

Different vanadia structures have been shown in the past to be present on the surface of supported vanadia catalysts depending on the vanadia loading [24,39,40]. In particular, in situ Raman spectroscopy studies have demonstrated that at submonolayer coverages vanadia exists on the titania surface in two forms: either as an isolated, vanadyl (VO_4) species or as a polymeric chain of these species. At low vanadia coverages, the Raman spectra of the vanadia catalysts exhibit a
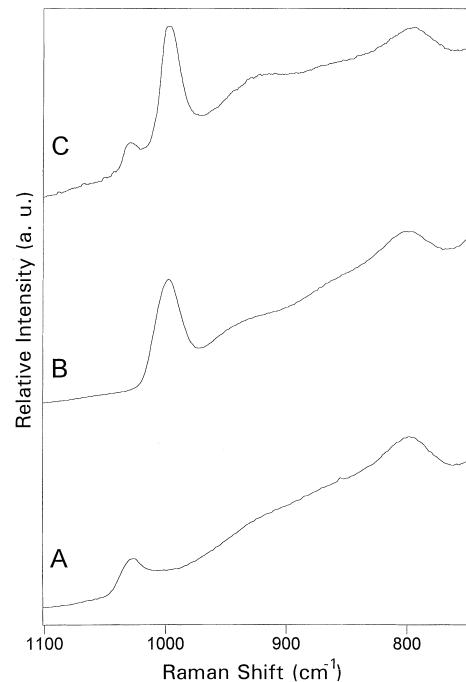
Fig. 1. Laser Raman spectra of the dehydrated: (a) V_2O_5/TiO_2, (b) MoO_3/TiO_2, and (c) V_2O_5–MoO_3/TiO_2 samples.

single sharp band at approximately 1027 cm^{-1}. This band has been assigned to the terminal V=O bond of the vanadyl structure. At higher coverages, the V=O band shifts to approximately 1030 cm^{-1} and a new broad band appears at approximately 930 cm^{-1}. This second Raman band has been assigned to the V–O–V bonds shared between the different vanadyl species in a polymeric chain. In agreement with these reports, the Raman spectrum of the dehydrated, unpromoted V_2O_5/TiO_2 catalyst (Fig. 1(a) and Fig. 2(a)) primarily shows a vanadia band at 1024 cm^{-1}, suggesting that most of the vanadia in this catalyst exists on the titania surface as an isolated species.

The presence of the metal oxide additives was found to have different effects on the Raman spectrum of vanadia depending on the nature of the additive. The two most effective promoters (MoO_3 and WO_3) exhibit their own Raman spectral features in the 750–1100 cm^{-1} region. The spectra of the MoO_3/TiO_2 and WO_3/TiO_2 samples are shown in Fig. 1(b) and Fig. 2(b), respectively, and exhibit characteristic Raman bands at 997 and 1011 cm^{-1}, which can be assigned to the surface molybdena and tungsta spe-
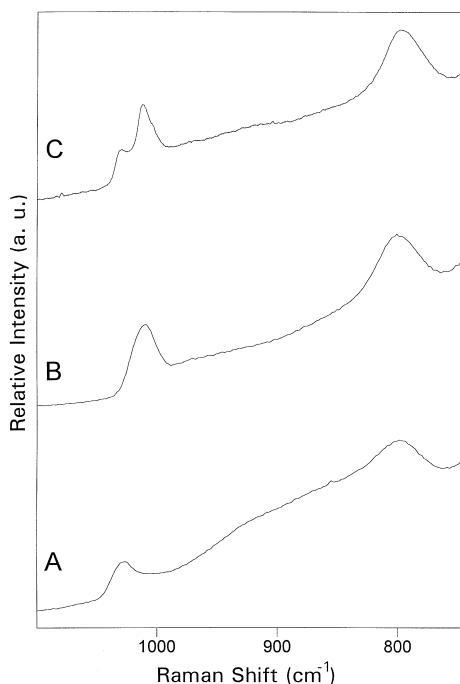
Fig. 2. Laser Raman spectra of the dehydrated: (a) V_2O_5/TiO_2, (b) WO_3/TiO_2, and (c) V_2O_5–WO_3/TiO_2 samples.

Fig. 3. Laser Raman spectra of the dehydrated: (a) V_2O_5–ZnO/ TiO_2, (b) V_2O_5–Nb_2O_5/TiO_2, (c) V_2O_5–Ga_2O_3/TiO_2, (d) V_2O_5– GeO_2/TiO_2, (e) V_2O_5–SnO_2/TiO_2, and (f) V_2O_5–CeO_2/TiO_2 samples.

cies, respectively, in agreement with previous literature reports [41,42]. The spectra of the promoted V_2O_5–MoO_3/TiO_2 and V_2O_5–WO_3/TiO_2 samples (Fig. 1(c) and Fig. 2(c), respectively) exhibit basically the same bands and at the same intensity with the single component samples (Fig. 1(a) and (b), Fig. 2(a) and (b)), suggesting that the structure of V_2O_5 and MoO_3/WO_3 are not significantly affected by the presence of each other. In addition, the broad band at 930 cm^{-1} appears to be present in the spectrum of the V_2O_5–MoO_3/TiO_2 sample, suggesting that a small fraction of the vanadia in this sample is in the polymeric form.

The remaining metal oxide additives utilized in this study exhibited no Raman spectral features of their own in the region of interest (750–1100 cm^{-1}), since they do not contain any M=O bonds in their structure, and single M–O bonds vibrate in the 400–700 cm^{-1} region [43]. Nb_2O_5 represents an exception because it contains a Nb=O bond, but its Raman signal is much weaker that those of other M=O bonds. The presence of most of the additives examined had no effect on the spectrum of V_2O_5/TiO_2, and the 1027 cm^{-1} band is

the only vanadia feature in the spectrum (Fig. 3(a)–(f)). On the contrary, in the spectra of the MnO_2- and Fe_2O_3-promoted samples (Fig. 4(a) and (b), respectively), in addition to the 1027 cm^{-1} band (which has slightly shifted in some of these spectra), there is also an evidence for the presence of the broad vanadia band at 930 cm^{-1}.

Finally, the presence of a new species with a broad Raman peak at approximately 1000 cm^{-1} is noted in the spectrum of the V_2O_5–La_2O_3/TiO_2 sample (Fig. 4(c)). No evidence for the presence of either the isolated or the polymeric vanadyl species can be found in this spectrum. An extensive characterization effort that could lead to the positive identification of the structure and origin of this new species is beyond the scope of the work described in this paper.

The Raman structural characterization results suggest two distinct models for the addition of the second metal oxide to the V_2O_5/TiO_2 system. In the first case, the presence of the second oxide (i.e. WO_3, ZnO, Nb_2O_5, Ga_2O_3, GeO_2, SnO_2 or CeO_2) does not appear
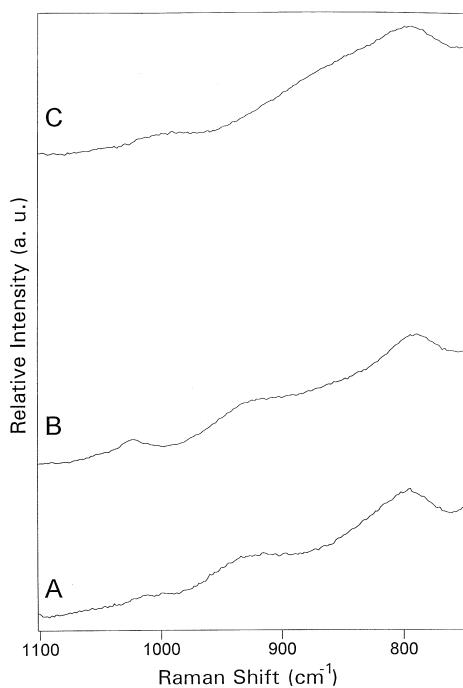
Fig. 4. Laser Raman spectra of the dehydrated: (a) V_2O_5–MnO_2/TiO_2, (b) V_2O_5–Fe_2O_3/TiO_2, and (c) V_2O_5–La_2O_3/TiO_2 samples.

to affect the structure of the surface vanadia species, which in the promoted samples remain primarily in the isolated monomeric form. Despite the structural similarity of the surface vanadia species however, the SCR activity of these samples varies significantly (Table 2). On the contrary, the addition of a metal oxide from the second group (i.e. MoO_3, MnO_2 or Fe_2O_3), appears to enhance the formation of the polymeric vanadyl species, raising the question of whether the activity differences of at least some of these samples may be explained in terms of the structural differences of vanadia. We have previously examined the effect of the vanadia coverage – and, thus, also structure – on the reactivity of V_2O_5/TiO_2 catalysts for the SCR reaction [32]. Under conditions similar to the ones employed in this work (i.e. in the presence of H_2O and SO_2), the SCR turnover frequency was found to decrease monotonically with the surface vanadia coverage. These previous observations, however, cannot account for the activity differences observed with the second group of promoted catalysts in the current study. Indeed, despite the fact that compared to the unpromoted sample, all of these catalysts had a higher

amount of polymeric vanadyl species (an effect similar to the one caused by an increased vanadia coverage), their SCR activity was found to be either higher (MoO_3), almost equal (Fe_2O_3), or lower (MnO_2) than the corresponding activity of the unpromoted sample. These observations lead to the conclusion that in the set of catalysts studied structural effects are not the dominating factor controlling SCR reactivity, in agreement with previous literature reports [24,34].

3.3. Vanadia reducibility

Hydrogen temperature programmed reduction (H_2-TPR) has been used in the past to probe the reducibility of vanadia in similar catalysts [12–14]. Its results however, should be viewed cautiously, since other factors – in addition to the reducibility of vanadia – could affect the location of the reduction peaks. Surface reduction for example, must be preceded by the dissociative adsorption of dihydrogen, and thus, could be affected by the equilibrium constant of hydrogen adsorption. Furthermore, it is possible that hydrogen atoms formed by the dissociation of dihydrogen on one metal oxide species may spill-over and reduce the second metal oxide. Finally, the surface mobility of atomic hydrogen may be different from the surface mobility of the intermediate species responsible for the vanadia reduction under SCR conditions.

As an alternative to H_2-TPR, NH_3-TPD was utilized in this study and the evolution of oxidation products was monitored as an indication of the onset of surface reduction reactions. The drawback of utilizing such an approach is that the desorption temperature of such products is also affected by the strength of their adsorption on the surface. The results of the NH_3-TPD experiments conducted over the catalysts employed in this study are summarized in Table 3. Of particular interest at this point are the peak temperatures for the desorption of water, which are indicative of the reduction of the surface. All samples examined exhibited two water desorption peaks: a low temperature one in the 488–538 K range and a high temperature peak in the 608–708 K range. The location of these peaks varied with sample composition indicating a change in surface redox properties as a result of the presence of the different promoters. No correlation was detected, however, between the

Table 3
NH$_3$-TPD results over various promoted V$_2$O$_5$/TiO$_2$ catalysts

Catalyst	n_{NH_3}[a] (µmol/g)	T_{NH_3}[b] (K)	T_{H_2O}[c] (K)
V$_2$O$_5$–Ga$_2$O$_3$/TiO$_2$	230	523	513, 643
V$_2$O$_5$–ZnO/TiO$_2$	230	488, 658	513, 638
V$_2$O$_5$–SnO$_2$/TiO$_2$	220	513, 683	528, 608
V$_2$O$_5$–Fe$_2$O$_3$/TiO$_2$	200	538, 703	VB[d], VB[d]
V$_2$O$_5$/TiO$_2$	180	503, 688	523, 613
V$_2$O$_5$–GeO$_2$/TiO$_2$	180	498, 623, 713	523, 633
V$_2$O$_5$–MnO$_2$/TiO$_2$	180	498, 643	533, 633
V$_2$O$_5$–Nb$_2$O$_5$/TiO$_2$	180	553, 688	523, 618
V$_2$O$_5$–WO$_3$/TiO$_2$	160	478, 713	518, 633
V$_2$O$_5$–CeO$_2$/TiO$_2$	130	523	508, VB[d]
V$_2$O$_5$–MoO$_3$/TiO$_2$	100	478, 623	523, 663
V$_2$O$_5$–La$_2$O$_3$/TiO$_2$	80	533	488, 708

[a]Total amount of adsorbed ammonia.
[b]Ammonia desorption peak temperatures.
[c]Water desorption peak temperatures.
[d]Desorption takes place over a broad temperature range, without a well-defined peak temperature.

maximum temperature of either of the two water desorption peaks and the SCR activity data. In addition to water, the presence of small amounts of nitrogen containing oxidation products (i.e. N$_2$, N$_2$O and NO$_2$) was also detected in the NH$_3$-TPD spectra of at least some of these samples. An attempt to correlate the desorption characteristics of these species with SCR activity was also unsuccessful.

Dumesic et al. [18] have demonstrated that a plethora of available kinetic and spectroscopic data for the SCR reaction over V$_2$O$_5$/TiO$_2$ catalysts can be explained by a relatively simple catalytic cycle:

$$NH_3 + M \Leftrightarrow NH_3-M \qquad (2)$$

$$NH_3-M + S \Leftrightarrow NH_3-S + M \qquad (3)$$

$$NH_3-S + NO \Rightarrow N_2 + H_2O + S' \qquad (4)$$

$$S' + O_2 \Rightarrow S \qquad (5)$$
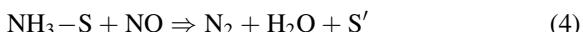
which includes the adsorption of ammonia on an acid site M (step 2); its activation on a vanadia site S (step 3); the reaction of the activated ammonia with gaseous or weakly adsorbed NO (accompanied by the reduction of the active vanadia site) (step 4); and finally, the reoxidation of the vanadia site by molecular oxygen (step 5). Under excess oxygen conditions, the available experimental evidence (i.e. independence of the

reaction rate from the oxygen concentration [25] and in situ characterization efforts that show vanadia to be primarily in the 5+ state [11,24]) suggest that step 5 is fast and kinetically insignificant. Furthermore, the near zero order dependence of the SCR rate on the ammonia concentration [25] suggests that the surface is almost saturated with ammonia and that step 2 is fast and close to equilibrium. A potential correlation between the SCR activity and the reducibility of vanadia in the promoted samples, would imply that step 4 is kinetically significant. The absence of such a correlation from the data presented above appears to suggest that this is not the case and led us to further consider the kinetic significance of step 3.

3.4. Surface acidity

Given the basic nature of the NH$_3$ molecule, acid surface sites are expected to be involved in steps 2 and 3 (sites M and S) of the proposed mechanism. The amount and strength of such sites in the promoted samples was probed by the use of NH$_3$-TPD. The results of these studies are summarized in Table 3.

NH$_3$ exhibits a bimodal desorption profile from the unpromoted V$_2$O$_5$/TiO$_2$ sample with peak maxima at 503 and 688 K. Integration of all desorption peaks corresponding to N-containing species indicates that under the adsorption conditions (i.e. 373 K and a gas phase consisting of 1000 ppm NH$_3$ in He) the NH$_3$ adsorption capacity of this sample is 180 µmol/g. This amount includes a small contribution from the desorption of nitrogen containing oxidation products. The results of Table 3 further indicate that the presence of the metal oxide additives affects both the number and the strength (as indicated by the shifts in the desorption peaks) of the surface acid sites. An attempt, however, to correlate the SCR activity with total acidity (as indicated by the NH$_3$ adsorption capacity of the promoted samples) was unsuccessful. Similarly, attempts to correlate the SCR activity with the position of the NH$_3$ desorption peaks and thus, the average strength of the acid sites were also proven unsuccessful.

Failure to correlate the SCR activity data with the total acidity of promoted V$_2$O$_5$/TiO$_2$ suggests that a special type of surface acid sites may be involved in the rate determining step of the SCR reaction. In fact, Topsøe et al. [11] have proposed that in the case of
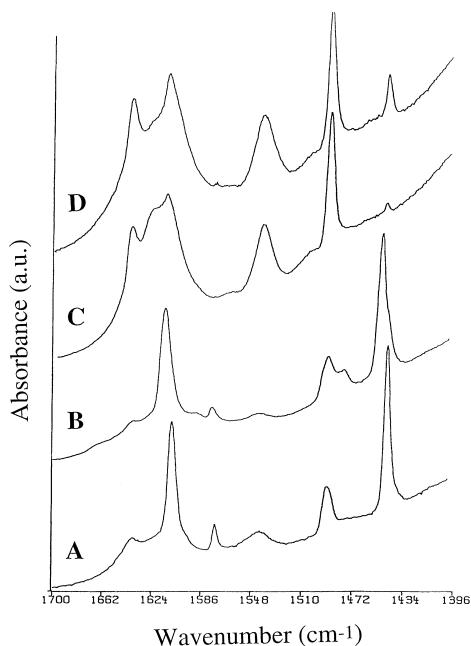
Fig. 5. DRIFTS spectra of pyridine adsorbed on: (a) V_2O_5/TiO_2, (b) V_2O_5–ZnO/TiO_2, (c) V_2O_5–MoO_3/TiO_2, and (d) V_2O_5–WO_3/TiO_2.

unpromoted V_2O_5/TiO_2 catalysts activation of the ammonia takes place on a Brønsted acid site. DRIFTS studies of adsorbed pyridine were utilized to determine the amount of surface Brønsted sites in the promoted samples, because the IR spectrum of chemisorbed pyridine is sensitive to the nature of the acid binding site and can clearly differentiate between the different types of surface acidity. Although this spectrum contains a number of peaks [44], two of them at approximately 1450 and $1540 \, cm^{-1}$ – assigned to unique modes of vibration of a pyridine complex coordinately bonded to a Lewis acid site and a pyridinium ion bonded to a Brønsted acid site, respectively, – are clearly separated from the rest and can be used for quantification of the two different types of acid sites.

The DRIFTS spectrum of pyridine adsorbed on the unpromoted V_2O_5/TiO_2 sample is shown in Fig. 5(a). In agreement with previous published reports [17], both Lewis and Brønsted acid sites are present on the surface of this sample. Furthermore, the intensity of the peak corresponding to pyridine coordinately bonded to a Lewis site ($1450 \, cm^{-1}$) is significantly

higher than the intensity of the peak corresponding to a pyridinium ion bonded to a Brønsted acid site ($1540 \, cm^{-1}$). This is also in agreement with previous studies [11] which have suggested that at low vanadia loadings the V_2O_5/TiO_2 catalysts exhibit a relatively small fraction of Brønsted acidity. The intensities of the two peaks characteristic of Brønsted and Lewis acid sites are affected significantly by the presence of the additive metal oxides, as shown in the other three spectra of Fig. 5. While the presence of ZnO appears to reduce the amount of Brønsted acidity (Fig. 5(b)), the presence of either MoO_3 or WO_3 results in a significant increase. A similar increase in Brønsted acidity with the addition of WO_3 to V_2O_5/TiO_2 was previously observed by Chen and Yang [21]. The origin and the location of these new Brønsted sites are not clearly understood at present. The spectrum of pyridine adsorbed on the V_2O_5–MoO_3/TiO_2 sample for example, shows Brønsted acidity comparable to the combined acidity of the MoO_3/TiO_2 and V_2O_5/TiO_2 samples, suggesting that in this case most of the new Brønsted sites in the promoted sample are associated with MoO_3. On the contrary, the spectrum of the V_2O_5–WO_3/TiO_2 sample shows more Brønsted acidity than the combined acidity of the WO_3/TiO_2 and V_2O_5/TiO_2 samples, suggesting that some new Brønsted sites may be generated due to the V_2O_5–WO_3 interaction.

The quantification of DRIFTS results presents some challenges associated with possible differences in sample morphology (e.g. density and surface area) and consistency in sample preparation (e.g. sample packing and surface geometry). The samples examined in this study were similar in morphology (including density and surface area) since the same TiO_2 support was used for all of them and constituted the majority component. Furthermore, the precision associated with the peak intensities of such measurements (which is affected by the consistency in sample preparation) has been established to be in the order of 10%, based on a large number of studies conducted within W.R. Grace's Analytical Division [45]. As a result, a quantitative comparison can be made among the relative amounts of surface Brønsted acid sites (obtained by integration of the area under the $1540 \, cm^{-1}$ peak) present on the different samples (Table 4). An attempt was then made to correlate the amount of surface Brønsted acidity with the

Table 4
Results of DRIFTS measurements of pyridine adsorption on various promoted V_2O_5/TiO_2 catalysts

Catalyst	Area of 1540 cm^{-1} peak (au)
V_2O_5–WO_3/TiO_2	0.10
V_2O_5–MoO_3/TiO_2	0.08
V_2O_5–Nb_2O_5/TiO_2	0.05
V_2O_5–GeO_2/TiO_2	0.04
V_2O_5/TiO_2	0.04
V_2O_5–Fe_2O_3/TiO_2	0.03
V_2O_5–CeO_2/TiO_2	0.03
V_2O_5–MnO_2/TiO_2	0.03
V_2O_5–SnO_2/TiO_2	0.02
V_2O_5–Ga_2O_3/TiO_2	0.01
V_2O_5–La_2O_3/TiO_2	0.01
V_2O_5–ZnO/TiO_2	0.00

SCR activity of the different promoted samples (Fig. 6). The results indicate a strong correlation between the amount of surface Brønsted acidity and the SCR activity. On the contrary, no such correlation was found between the amount of Lewis acidity and the SCR activity.

From a mechanistic standpoint, this result indicates that a Brønsted acid site is involved in the rate determining step of the SCR reaction. Based on all arguments presented so far, and under the conditions employed in this study, this is believed to be the activation of ammonia shown as step 3 in the mechanism presented previously. A similar conclusion was also reached by Topsøe et al. [11] based on the study of V_2O_5/TiO_2 catalysts of variable vanadia loading. The confirmation of this conclusion by the use of the metal oxide additives, however, raises some questions regarding the nature and location of the Brønsted sites participating in the reaction. It is clear that in addition to a Brønsted acid site, a reducible vanadia site is needed for the NO–NH_3 reaction described as step 4 in the reaction mechanism (both the MoO_3/TiO_2 and WO_3/TiO_2 samples for example, exhibit Brønsted acidity similar to or higher than this of the V_2O_5/TiO_2 sample but very low SCR activity). Topsøe et al. proposed that the Brønsted acidity is directly associated with the active reducible vanadia site. Although this is probably the case with the unpromoted V_2O_5/TiO_2 catalysts, it may not be necessarily true for the promoted samples. From the results obtained with these samples, it appears that the presence of a Brønsted acid site in close proximity with the vanadia site results in a promoting effect on SCR activity. Such a conclusion also hints that the intermediate species involved in SCR (i.e. the activated ammonia species) may have a higher surface mobility than previously anticipated.
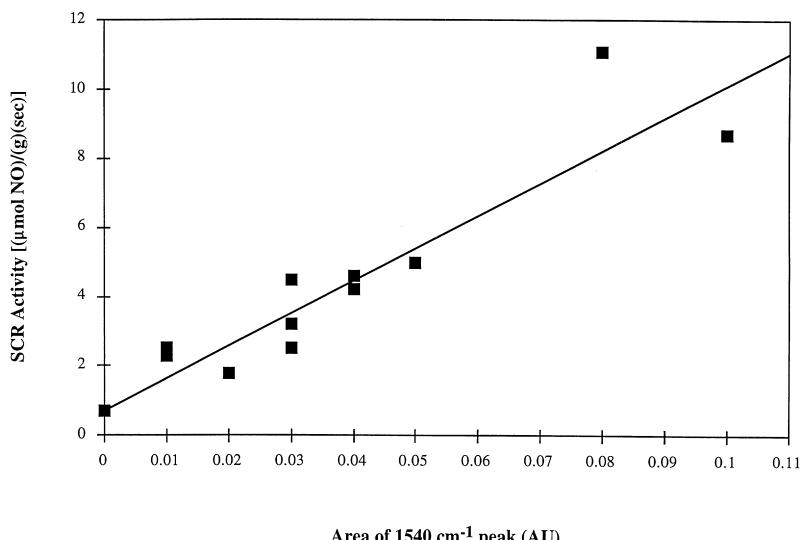
Fig. 6. SCR activity as a function of the Brønsted acidity for various promoted V_2O_5/TiO_2 catalysts.

4. Conclusions

A systematic investigation of the effect of various metal oxides additives on the reactivity of a 1 wt% V_2O_5/TiO_2 catalyst was carried out under conditions similar to the ones encountered in commercial applications and revealed the significant effect of such additives on the rate of the selective catalytic reduction (SCR) of NO by NH_3. An extensive characterization effort was then undertaken in an attempt to correlate the structure and chemical properties of the promoted catalysts with their SCR reactivity. The results of this effort indicate that the presence of the additive metal oxides may affect a variety of catalyst properties, including the structure and reducibility of vanadia, and the overall amount and type of surface acidity. Among these factors the only one that correlates with SCR reactivity is the amount of surface Brønsted acidity. Consequently, an increase in the number of Brønsted acid sites on the catalyst surface results in an increase in the SCR rate. These observations appear to be in agreement with the four step mechanism proposed by Dumesic et al. [18]. They further suggest that under the conditions studied, the activation of ammonia on a Brønsted acid site controls the reaction rate.

Acknowledgements

References

[1] H. Bosch, F. Janssen, Catal. Today 2 (1988) 369.
[2] C.J. Pereira, M.D. Amiridis, ACS Symp. Ser. 587 (1995) 1.
[3] S.M. Cho, Chem. Eng. Prog. 90 (1994) 39.
[4] P. Forzatti, L. Lietti, Heter. Chem. Rev. 3 (1996) 33.
[5] M. Takagi, T. Kawai, M. Soma, T. Onishi, K. Tamaru, J. Catal. 57 (1979) 528.
[6] J.A. Odriozola, H. Heinemann, G.A. Somorjai, J.F.G. de la Banda, P. Pereira, J. Catal. 119 (1989) 71.
[7] G.T. Went, L.-J. Leu, R.R. Rosin, A.T. Bell, J. Catal. 134 (1992) 492.
[8] M. Inomata, A. Miyamoto, Y. Murakami, J. Catal. 62 (1980) 140.
[9] F.J.J.G. Janssen, F.M.G. van der Kerkhof, H. Bosch, J.R.H. Ross, J. Phys. Chem. 91 (1987) 5921.
[10] G. Ramis, G. Busca, V. Lorenzelli, P. Forzatti, Appl. Catal. 64 (1990) 243.
[11] N.-Y. Topsøe, J.A. Dumesic, H. Topsøe, J. Catal. 151 (1995) 241.
[12] G. Ramis, G. Busca, F. Bregani, P. Forzatti, Appl. Catal. 64 (1990) 259.
[13] L. Lietti, J. Svachula, P. Forzatti, G. Busca, G. Ramis, F. Bregani, Catal. Today 17 (1993) 131.
[14] J. Nickl, D. Dutoit, A. Baiker, U. Scharf, A. Wokaum, Ber. Bunsenges. Phys. Chem. 97 (1993) 217.
[15] R.A. Rajadhyaksha, H. Knozinger, Appl. Catal. 51 (1989) 81.
[16] J.P. Chen, R.T. Yang, J. Catal. 125 (1990) 411.
[17] N.-Y. Topsøe, J. Catal. 128 (1991) 499.
[18] J.A. Dumesic, N.-Y. Topsøe, T. Slabiak, P. Morsing, B.S. Clausen, E. Törnqvist, H. Topsøe, Proceedings of the 10th International Congress on Catalysis, Budapest, 1993, p. 1325.
[19] E. Hums, G.W. Spitznagel, ACS Symp. Ser. 587 (1995) 42.
[20] G. Tuenter, W.F.V. Leeuwen, L.J.M. Snepvangers, Ind. Eng. Chem. Prod. Res. Dev. 25 (1986) 633.
[21] J.P. Chen, R.T. Yang, Appl. Catal. 80 (1992) 135.
[22] G.W. Spitznagel, K. Hüttenhofer, J.K. Beer, ACS Symp. Ser. 552 (1994) 172.
[23] R.-Y. Weng, J.-F. Lee, Appl. Catal. 105 (1993) 41.
[24] I.E. Wachs, G. Deo, B.M. Weckhuysen, A. Andreini, M.A. Vuurman, M. de Boer, M. Amiridis, J. Catal. 161 (1996) 211.
[25] J. Marangozis, J. Ind. Eng. Chem. Res. 31 (1992) 987.
[26] H.G. Lintz, T. Turek, Appl. Catal. A 85 (1992) 13.
[27] J.A. Dumesic, N.-Y. Topsøe, H. Topsøe, Y. Chen, T. Slabiak, J. Catal. 163 (1996) 409.
[28] J.W. Beeckman, L.L. Hegedus, Ind. Eng. Chem. Res. 30 (1991) 969.
[29] N. Wakao, J.M. Smith, Chem. Eng. Sci. 17 (1962) 825.
[30] J.W. Beeckman, Ind. Eng. Chem. Res. 30 (1991) 428.
[31] M.D. Amiridis, J.P. Solar, Ind. Eng. Chem. Res. 35 (1996) 978.
[32] M.D. Amiridis, I.E. Wachs, G. Deo, J.-M. Jehng, D.S. Kim, J. Catal. 161 (1996) 247.
[33] S. Morikawa, H. Yoshida, H. Takahashi, S. Kurita, Chem. Lett. 251 (1981).
[34] A. Andreini, M. de Boer, M.A. Vuurman, G. Deo, I.E. Wachs, J. Chem. Soc., Faraday Trans. 92 (1996) 3267.
[35] H. Matralis, S. Theret, S. Bastians, M. Ruwet, P. Grange, Appl. Catal. B 5 (1995) 271.
[36] I. Nova, L. Lietti, L. Casagrande, L. Dall'Acqua, E. Giamello, P. Forzatti, Appl. Catal. B 17 (1998) 245.
[37] F. Hilbrig, H. Schmelz, H. Knozinger, M. Sinev, A.T. Bell, M. Schmal, P. Forzatti, I.E. Wachs, T. Uematsu, J.C. Vedrine, E. Hums, Stud. Surf. Sci. Catal. 75 (1993) 1351.
[38] L. Lietti, J. Svachula, P. Forzatti, G. Busca, G. Ramis, F. Bregani, Catal. Today 17 (1993) 131.
[39] I.E. Wachs, J. Catal. 124 (1990) 570.

[40] G.T. Went, L.-J. Leu, A.T. Bell, J. Catal. 134 (1992) 479.
[41] M.A. Vuurman, I.E. Wachs, J. Phys. Chem. 96 (1992) 5008.
[42] M.A. Vuurman, I.E. Wachs, A.M. Hirt, J. Phys. Chem. 95 (1991) 9928.
[43] M.A. Vuurman, D.J. Stufkens, A. Oskam, G. Deo, I.E. Wachs, J. Chem. Soc., Faraday Trans. 92 (1996) 3259.
[44] E.P. Parry, J. Catal. 2 (1963) 371.
[45] L.B. Peters, J.B. Lynch, W.-C. Cheng, Grace Analytical News 19 (1992) 5.